LLNL Identification Program: Regional Body-wave Correction Surfaces and Surface-wave Tomography Models to Improve Discrimination

W.R. Walter, A.J. Rodgers, M.E. Pasyanos, K.M. Mayeda, A. Sicherman, and D.B. Harris

U.S. Department of Energy

Lawrence
Livermore
National
Laboratory

July 27, 2001

DISCLAIMER

This document was prepared as an account of work sponsored by an agency of the United States Government. Neither the United States Government nor the University of California nor any of their employees, makes any warranty, express or implied, or assumes any legal liability or responsibility for the accuracy, completeness, or usefulness of any information, apparatus, product, or process disclosed, or represents that its use would not infringe privately owned rights. Reference herein to any specific commercial product, process, or service by trade name, trademark, manufacturer, or otherwise, does not necessarily constitute or imply its endorsement, recommendation, or favoring by the United States Government or the University of California. The views and opinions of authors expressed herein do not necessarily state or reflect those of the United States Government or the University of California, and shall not be used for advertising or product endorsement purposes.

This is a preprint of a paper intended for publication in a journal or proceedings. Since changes may be made before publication, this preprint is made available with the understanding that it will not be cited or reproduced without the permission of the author.

This report has been reproduced
directly from the best available copy.

Available to DOE and DOE contractors from the
Office of Scientific and Technical Information
P.O. Box 62, Oak Ridge, TN 37831
Prices available from (423) 576-8401
http://apollo.osti.gov/bridge/

Available to the public from the
National Technical Information Service
U.S. Department of Commerce
5285 Port Royal Rd.,
Springfield, VA 22161
http://www.ntis.gov/

OR

Lawrence Livermore National Laboratory
Technical Information Department's Digital Library
http://www.llnl.gov/tid/Library.html

LLNL IDENTIFICATION PROGRAM: REGIONAL BODY-WAVE CORRECTION SURFACES AND SURFACE-WAVE TOMOGRAPHY MODELS TO IMPROVE DISCRIMINATION

William R. Walter, Arthur J. Rodgers, Michael E. Pasyanos, Kevin M. Mayeda,
Alan Sicherman and David B. Harris

Lawrence Livermore National Laboratory

ABSTRACT

LLNL identification research is focused on the problem of correctly discriminating small-magnitude explosions from a background of earthquakes, mining tremors, and other events. The goal is to reduce the variance within the population of each type of event, while increasing the separation between the explosions and the other event types. We address this problem for both broad categories of seismic waves: body waves and surface waves. First, we map out the effects of propagation and source size in advance so that they can be accounted for and removed from observed events. This can dramatically reduce the population variance. Second, we try to optimize the measurement process to improve the separation between population types.

For body waves we focus on the identification power of the short-period regional phases Pn, Pg, Sn and Lg, which can often be detected down to very small magnitudes. Many studies have shown that particular ratios of these phases, such as 6- to 8-Hz Pn/Lg, can effectively discriminate between closely located explosions and earthquakes. To extend this discrimination power over broad areas, we use our revised Magnitude and Distance Amplitude Correction (MDAC2) procedure. This joint source and path model fits the observed spectra and removes magnitude and distance trends from the data. The MDAC residuals are kriged to provide full 2-D path corrections by phase and frequency band. The MDAC residuals allow the exploration of all possible ratios and multivariate combinations of ratios for their discrimination power. We also make use of the MDAC spectra and the noise spectra to determine the expected detectability of each phase and use that to optimize the multivariate discriminants as a function of location. We quantify the discrimination power using the misidentified event trade-off curves and an equi-probable measure. We evaluate the correction surfaces using a cross-validation technique. The result is an end-to-end validation and discrimination performance measure for each station analyzed, and a set of measurement algorithms and correction surfaces that greatly improves discrimination.

For surface waves we continue to make improvements in our regional group velocity tomography models. We have recently expanded our Rayleigh and Love wave dispersion measurements from the Middle East and North Africa into the European Arctic. The resulting tomography models now cover all of western Eurasia and provide high-resolution maps of group velocity from 10- to 100-seconds period. The maps also provide estimates of the expected phase spectra of new events that can be used in phase-match filters to compress the expected signals and improve the signal-to-noise ratio on surface wave magnitude (Ms) estimates. Phase match filters in combination with regional Ms formulas can significantly lower the threshold at which Ms can be measured, extending the Ms-mb discriminant. We have measured Ms in western Eurasia for thousands of events at tens of stations, with and without phase match filtering, and found a marked improvement in discrimination. Finally we are exploring the Ms-yield relation for the explosions in the dataset with announced yields.

KEY WORDS: seismic, regional, discrimination, identification, explosion

OBJECTIVES

Monitoring the world for potential nuclear explosions requires characterizing seismic events and discriminating between natural and man-made seismic events, such as earthquakes and mining activities, and nuclear weapons testing. We are developing, testing, and refining size-, distance-, and location-based regional seismic amplitude corrections to facilitate the comparison of all events that are recorded at a particular seismic station. These corrections, calibrated for each station, reduce amplitude measurement scatter and improve discrimination performance. We test the methods on well-known (ground truth) datasets in the U.S. and then apply them to the uncalibrated stations in Eurasia, Africa, and other regions of interest to improve underground nuclear test monitoring capability.

RESEARCH ACCOMPLISHED

As part of the overall National Nuclear Security Administration Ground-based Nuclear Explosion Monitoring (GNEM) Research and Engineering program, we continue to pursue a comprehensive research effort to improve our capabilities to seismically characterize and discriminate underground nuclear tests from other natural and man-made sources of seismicity. To reduce the monitoring magnitude threshold, we make use of regional body and surface wave data to calibrate each seismic station. Our goals are to reduce the variance and improve the separation between earthquakes and explosion populations by accounting for the effects of propagation and differential source size. Here, we briefly review two of these efforts: 1) MDAC2 - a revised spectral fitting technique to improve regional body-wave discrimination and 2) high-resolution surface wave tomography to provide structural information in aseismic regions and to improve Ms:mb discrimination.

MDAC2

Effective earthquake-explosion discrimination has been demonstrated in a broad variety of studies using ratios of regional amplitudes in high-frequency (primarily 1-to 20-Hz) bands. When similar-sized earthquakes and explosions are nearly co-located, we can understand the observed seismic contrasts, such as the relative P-to-Lg excitation, in terms of depth, material property, focal mechanism and source time function differences. However, the availability of reference earthquakes, and particularly nuclear tests, to compare to a new event in question is highly non-uniform and limited. Therefore, in real monitoring cases, we are often interested in comparing events that are not co-located and may have quite different sizes. In order to make sure any observed differences between a new event in question and the reference events (or models) are not due to differences in path or magnitude, we must correct for these effects.

For the past several years we have been working with our colleagues at Los Alamos National Laboratory on the best ways to model and remove magnitude and distance trends from regional amplitudes. The original MDAC (Magnitude and Distance Amplitude Correction) procedure involved estimating and removing a simple theoretical earthquake spectrum from the data to remove any magnitude and distance trends in the regional phase amplitudes and any discriminants formed from those amplitudes (Taylor et al., 2002). Recently, we have refined and improved the procedure by generalizing the source model, taking advantage of independent moment estimates and reducing some of the free parameters (Walter et al., 2001, Walter and Taylor, 2001.

The source spectrum depends upon the seismic moment and stress drop and can have additional complications due to non-constant stress drop scaling and differential P/S corner frequency effects. We require the different phases for the same event recorded at the same station to have the same moment and apparent stress (or stress drop) values and other source parameters, such as corner frequencies to be related to each other. This requirement effectively imposes some of the ratio constraints discussed in Rodgers and Walter (2002) on the amplitudes and improves discrimination performance. While such models of source spectra are certainly oversimplified, they have proven track records of providing good first-order fits to real earthquakes. In addition they also provide simple theoretical models to use in aseismic areas.

The MDAC formulation was revised in two ways:

1. We take advantage of the very stable moment magnitude determinations from regional coda envelopes (see Myers et al., this Proceedings). The coda-based technique provides an accurate and independent estimate

of moment from just one station. Using a direct measure of moment also eliminates the need to scale from other magnitudes such as m_b to moment eliminating two fitting parameters from the original formulation (Taylor et al, 2002). The combination of using the more stable coda measure and eliminating two free parameters should reduce scatter in the resulting correction.

2. We generalize the Brune (1970) source spectrum to allow for arbitrary stress scaling and P to S corner frequency ratios. A problem with non-constant stress drop scaling is that the Brune (1970) model is specifically set up as a constant stress drop model. Taylor et al. (2002) have implemented a non-constant scaling, but at a cost of the stress drop becoming a non-physical parameter. This means we can no longer interpret a stress drop in terms of bars (or MPa) in the non-constant scaling case. This is somewhat unsatisfactory both theoretically and practically when we want to use the MDAC formulation in regions without data where parameters like stress drop may be determined from models. Allowing variable P to S corner frequency ratios is also supported by some earthquake studies and gives greater flexibility to the spectral fitting.

The details of the MDAC2 formulation are given in Walter and Taylor (2001). The predicted spectrum is a convolution of the revised source terms and the previously used geometrical spreading, site, and apparent attenuation terms. We can write the log of the MDAC2 predicted spectrum as (Walter and Taylor, 2001):

$$\log P(f,R) = \log(S_o) - \log\left(1 + \left(\frac{\omega}{\omega_c}\right)^2\right) + \log G(R) + Site(f) - \frac{\pi R}{Q_o c} f^{(1-\gamma)} \log(e) \qquad (1)$$

for a regional phase with velocity c. Here S_o is the source low-frequency spectral level and Q_o is the source corner frequency. These terms are set by the input moment, the apparent stress scaling and material property terms. Apparent stress, geometrical spreading $(G(R))$, site effect, and attenuation (Q_o, γ) terms are typically solved for using a grid search technique that simultaneously minimizes the spectral fit residual and residual magnitude and distance trends. In this way *a priori* information such as previous studies on geometrical spreading or Q-tomography results can be easily incorporated. Finally we can further reduce the MDAC2 residual amplitude variance by using the Bayesian kriging method of Schultz et al (1998) on the results.

Nevada Test Site Examples

The availability in the Western U.S. of many good regional records of earthquakes and nuclear explosions, and much *a priori* information on attenuation and geometrical spreading, make it a good place to test out the MDAC spectral fitting. We use our own geometrical spreading (critical distance R_o, distance exponent η) and attenuation values, which are very similar to those found in prior studies (e.g. Chavez and Priestly, 1986). They are shown in the table below:

Phase	R_o	η	Q_o	γ
Pn	0	1.1	210	.65
Pg	100.	0.5	190	.45
Lg	100.	0.5	200	.54

An example of the MDAC2 simultaneous fit to Pn, Pg and Lg spectra is shown in Figure 1 for the Little Skull Mountain earthquake mainshock recorded at station KNB in Utah about 300 km distant. This earthquake occurred on the Nevada Test Site (NTS) in June of 1992 with a good aftershock sequence and is only a few tens of kilometers away from the sites of many previous nuclear tests. This figure shows the effect on the spectral fitting of the variable P to S corner frequency ratio. The left hand plot is for equal corner frequency values while the right hand plot is for high P corner frequency by the ratio of the wave velocities (1.73). The best fit appears to be closer to equal corner frequency values.

**MDAC2 fit to Mw=5.68 Little Skull Mountain earthquake
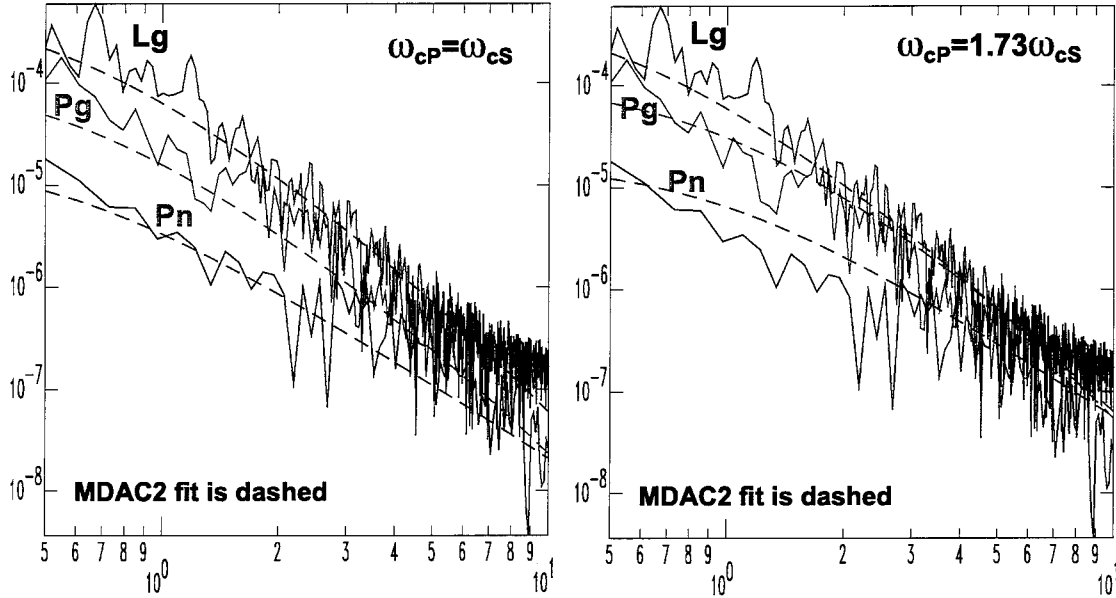for two different P/S corner frequency values**

Figure 1. MDAC2 fit to Mw=5.68 Little Skull Mountain earthquake for two different P/S corner frequency values.

Another example of MDAC2 scaling is shown in Figure 2. Here we show Lg spectra for the Little Skull Mountain mainshock and two aftershocks. The coda moment magnitudes are from a previous study (Mayeda and Walter, 1996). Note that the constant apparent stress model on the left does not fit the data as well as the stress scaling with $M_o^{1/4}$ shown on the right. This is consistent with our previous spectral studies using corrected coda envelope measure(Mayeda and Walter, 1996).

One of the major reasons that removing trends from the regional amplitude and discriminant ratios is important is to facilitate the creation of multivariate discriminants. This is the optimal combination of two or more specific amplitude ratios ("features") to improve discrimination. Several studies have shown that the combination of two mediocre discrimination ratios can surprisingly improve performance (e.g. Taylor, 1996). The reason is that combining more features brings more independent information to bear on the problem and also takes advantage of hidden favorable correlation structure between measures. For example, we show in Figure 3 some combinations of three discriminant measures from a previous study (Walter et al., 1995) for NTS.

The magnitude dependent effect of corner frequency scaling is particularly apparent in the Lg coda spectral ratio in Figure 3. We remove this prior to combining ratios. To measure the discrimination performance, we calculate receiver-operator curves (ROC), which can be thought of as the error rates when moving a constant decision line through all possible values. These ROC curves give the tradeoff in performance between the type 1 error (misidentified explosion as an earthquake) and type 2 error (misidentified earthquake as an explosion). A single metric is then given by the equi-probable value, which is defined as the error (point on the ROC curve) where the error rates are equal. In Figure 3 we can see that the best individual ratio is 6-8 Hz Pn/Lg with an equi-probable values of about 2.5%. Surprisingly, though using a linear discriminant analysis (LDA), combination of the two mediocre discriminants 6-8 Hz Pg/Lg and 1-2 Hz to 6-8 Hz Lg coda out-performs the 6-to 8-Hz Pn/Lg. This demonstrates the need to calibrate multivariate discriminants before choosing particular combinations and assessing performance.

An example of MDAC2 fits to Lg spectra from the 1992 Little Skull Mountain sequence at the Nevada Test Site: Mainshock and two aftershocks.
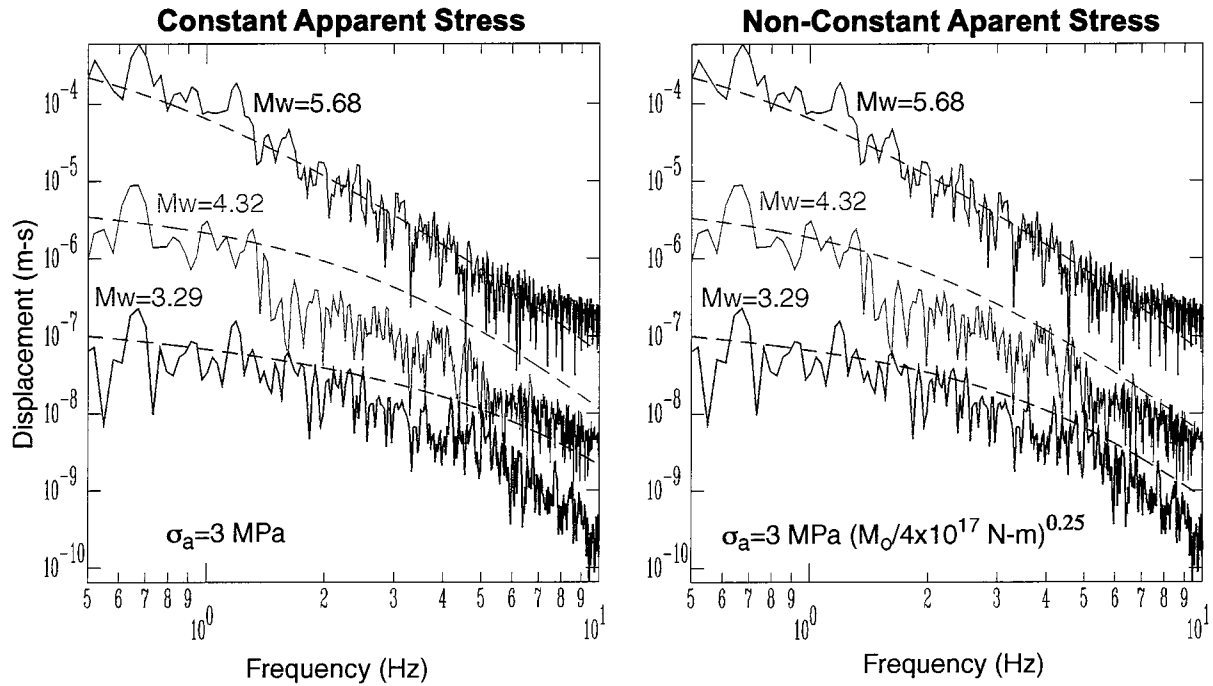

Figure 2. . Example of MDAC2 fits to Lg spectra for constant and non-constant apparent stress cases.
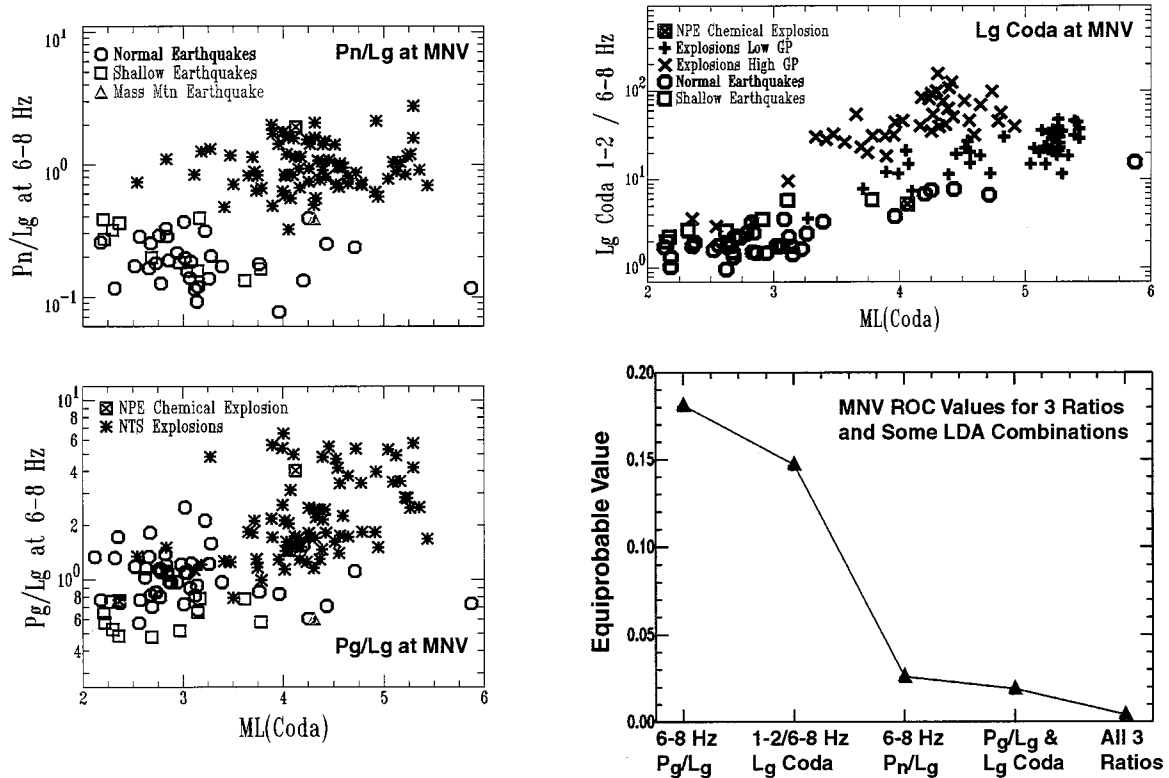
Figure 3. Examples of improving discriminant performance by combining individual measures. Color scatter plots show individual discriminant measures from Walter et al (1995). The lower right figure shows the performance, as measured by equi-probable value, of these individual measures and LDA combinations of them.

An additional consideration in deciding which regional amplitudes to use for individual or multivariate discrimination is their detectability in the frequency bands of interest at a given station. We can use the MDAC2 formulation to estimate this as well as discussed in the paper by Harris et al. (this Proceedings).

Surface Wave Tomography

For the past several years, we have been making regional surface wave group velocity measurements in western Eurasia with the goal of creating a high-resolution tomography model. Such tomography models provide information on velocity structure over broad areas and particularly in aseismic regions such as North Africa and stable Eurasia (e.g. Ritzwoller and Levshin, 1998; Pasyanos et al., 2001a). Last year, we reported on tomography results in the Middle East and North Africa. This year, we have extended the model north to include all of Western Eurasia. In addition, following the guidelines for measurements laid out in the 1998 surface wave workshop (Walter and Ritzwoller, 1998) we have exchanged group velocity curves with groups at the University of Colorado and SAIC/Maxwell. The tomography maps that we have created are thus formed from both our own regional measurements and the broader measurements provided by those two groups. Overall, we have examined more than 20,000 seismograms and made more than 9900 Rayleigh wave measurements and 5400 Love wave measurements at periods from 10-100 seconds. These numbers apply to the middle period range and the number of good measurements decreases at the shorter and longer periods. In addition we have incorporated more than 3000 path measurements from the University of Colorado (Ritzwoller, written communication) and SAIC/Maxwell (Stevens, written communication). An example of the event-station paths measured and the tomography results is shown in Figure 4 for Rayleigh waves at 20-seconds period.

The tomography models can be used to estimate velocity structure directly by inversion. However, because surface waves are most sensitive to S-wave velocities averaged over some depth range, these estimates of P-wave velocity structure can be quite non-unique. To better resolve surface wave inversion trade-off issues, we have recently performed constrained grid searches using these tomography models and incorporating other datasets (e.g. Pn tomography, receiver functions) and *a priori* information (e.g. sediment models, Poisson ratios) to estimate velocity structure (Pasyanos and Walter, 2001). Finally, the surface wave tomography results provide a means to test *a priori* geophysical models and we explore this idea more fully in Pasyanos et al., 2001b, on a Western Eurasia and North Africa (WENA) model. Tests of this *a priori* WENA model for improving location are discussed in Schultz et al. (this Proceedings).

20 Second Rayleigh Wave Tomography

Paths

Model

2.58 2.68 2.79 2.87 2.94 3.01 3.07 3.14 3.22 3.34 3.65
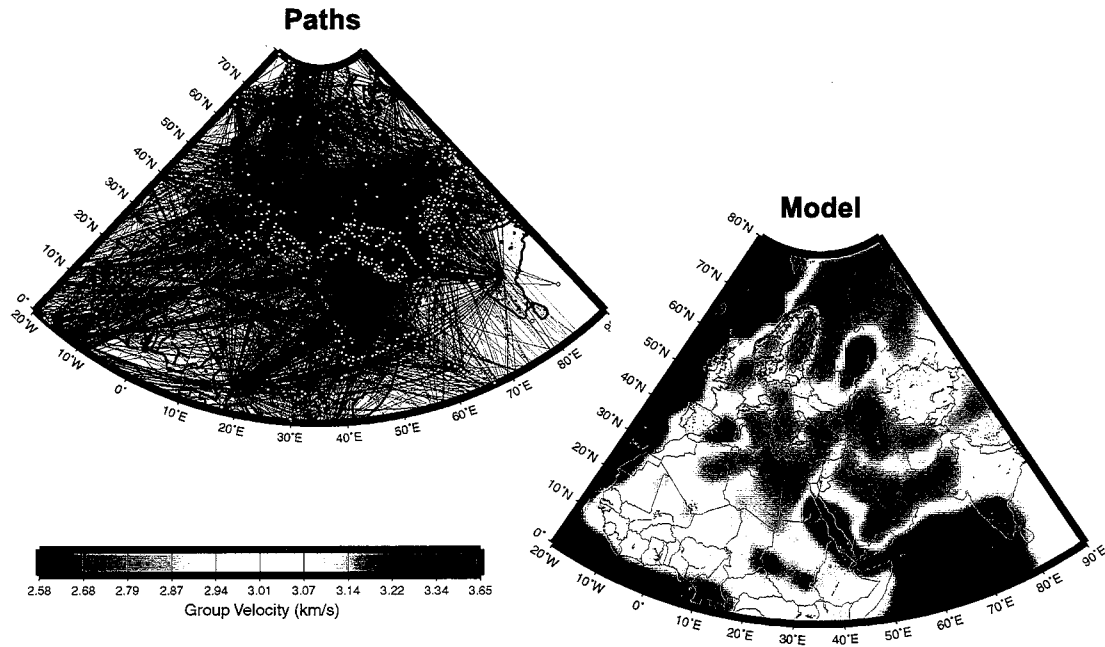Group Velocity (km/s)

Figure 4. Example of tomography input and results at 20-s period. Top plot shows the events (yellow circles), stations (red triangles) and paths (blue lines) used in the tomography. The path coverage is fairly good in most of the plot, but there are some holes without many crossing paths around the periphery of the plot. The model plot shows the 20-s group velocity. The slower regions match up well with known sedimentary basins and tectonic regions. The faster regions correspond well with oceanic regions and exposed cratons.

Phase-matched M_S and Regional M_S-m_b

The teleseismic discriminant M_S:m_b is one of the best understood and most effective discriminants known (e.g. Stevens and Day, 1985). Several studies have also shown that it appears to be effective down to as small magnitudes as can be measured regionally (e.g., Denny et al., 1987). The problem is that the 20-second surface wave amplitude on which M_S is based can be below the noise even at regional distances. We are researching several ways to allow M_S measurements on smaller magnitude events to be made and used to improve discrimination. One way is to allow regional M_S measurements at periods between 10 and 20 s where the regional Airy phase produces the largest amplitudes (e.g., Denny et al., 1987). Additionally we can improve signal-to-noise by making use of phase-match filters (e.g. Herrin and Goforth, 1977). This is particularly attractive because in addition to reducing the noise level in the signal, it can provide an accurate maximum Ms estimate even on a very noisy trace. For small explosions that have reduced M_S excitation to start with and may not have observable surface waves, this method can still provide some discrimination power relative to earthquakes of the same mb that do have measurable M_S.

The Rayleigh wave group velocity tomography described above can be used to provide predicted group velocity curves for input to a phase-match filtering routine. We can pre-calculate the expected group velocity at a station for any nearby event using the tomography model. In Figure 5, we show such a surface for station KEV in Norway. In addition we can use the measurements to provide an additional refinement to the model predictions using an intelligent interpolation technique. Here we use the Bayesian kriging technique of Schultz et al. (1998) on the measured residuals and add these back to the surface. Pasyanos (2000) previously demonstrated that this model plus a kriging approach provides better estimates of group velocity than either the model or kriging alone. Figure 5 shows an example of a PDE explosion and compares the raw data, a bandpass-

filtered signal and a redispersed seismogram from a phase-match filter. Note the improved signal-to noise in the phase-match trace. We previously have compared the impact on the Ms mb discriminant of using phase-match Ms estimates instead of the normal filters in the Middle East and North Africa and found significant improvement. We are now recalculating this comparison for the much larger western Eurasian dataset and will report on Ms:mb results at the meeting
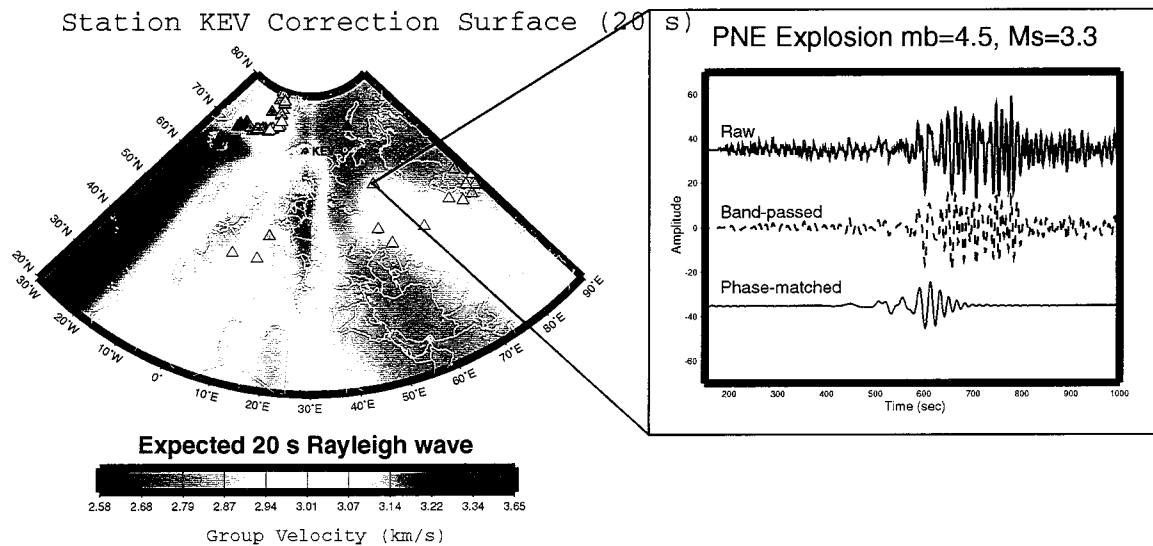

Figure 5. Correction surface for KEV showing predicted 20 second Rayleigh group velocities as a function of event location. The inset compares the results of three different processing on a PNE seismogram. The phase-match redispersed seismogram result comes from using the correction surface.

CONCLUSIONS AND RECOMMENDATIONS

Regional discrimination algorithms require calibration at each seismic station to be used for nuclear explosion monitoring. We have developed a revised Magnitude and Distance Amplitude Correction procedure to remove source size and path effects from regional body-wave phases. This allows the comparison of any new regional events recorded at a calibrated station with all available reference data and models. This also facilitates the combination of individual measures to form multivariate discriminants that can have significantly better performance. We have also developed surface wave group velocity maps and correction surfaces for phase-match filtering to improve Ms-mb discrimination and lower its effective threshold. Calibrating seismic stations to monitor for nuclear testing is a challenging task that will require processing large amounts of data, and collaboration with government, academic and industry researchers and incorporation of the extensive R&D results both within and outside of NNSA.

REFERENCES

Brune, J., (1970). Tectonic stress and the spectra from seismic shear waves earthquakes, *J. Geophys. Res.*, **75**, 4997-5009.

Chavez, D., and K. F. Priestley (1986). Measurement of frequency dependent Lg attenuation in the Great Basin, *Geophys. Res. Lett.*, *13*, 551-554.

Denny, M. D., S. R. Taylor, and E. S. Vergino (1987). Investigation of mb and Ms formulas for the western United States and their impact on the Ms/mb discriminant, Bull. Seism. Soc. Am., 77, 987-995.

Herrin, E. and T. Goforth (1977). Phase-matched filters: Applications to the study of Rayleigh waves, *Bull. Seism. Soc. Amer., 67*, 1259-1275.

Mayeda, K. M. and W. R. Walter, (1996). Moment, energy, stress drop and source spectra of Western U.S. earthquakes from regional coda envelopes, *J. Geophys. Res., 101*, 11,195-11,208.

Pasyanos, M. E. (2000). Predicting geophysical measurements: testing a combined empirical and model-based approach using surface waves, *Bull. Seism. Soc. Am., 90*, 790-796.

Pasyanos, M. E., and W. R. Walter (2001b). Crust and upper mantle structure of North Africa, Europe and the Middle East from inversion of surface waves, *Geophys. J.* (in revision).

Pasyanos, M. E., W. R. Walter and S. E. Hazler (2001a). A surface wave dispersion study of the Middle East and North Africa for monitoring the comprehensive nuclear-test-ban treaty, *Pure. Appl. Geophys., 158*, 1145-1474.

Pasyanos, M. E., W. R. Walter, M. Flanagan, P. Goldstein, and J. Bhattacharyya (2001b). Building and testing a geophysical model for Western Eurasia and North Africa, *J. Geophys. Res.* (submitted).

Ritzwoller, M. H., and A. L. Levshin (1998). Eurasian surface wave tomography: group velocities, *J. Geophys. Res.* 103,4839-4878.

Rodgers, A. J. and W. R. Walter, (2002). Seismic Discrimination of the May 11, 1998 Indian Nuclear Test with Short-Period Regional Data From Station NIL (Nilore, Pakistan), *Pure Appl. Geophys.* (in press).

Schultz, C, S. Myers, J. Hipp, and C. Young (1998). Nonstationary Bayesian kriging: a predictive technique to generate corrections for detection, location and discrimination, *Bull. Seism. Soc. Am., 88* 1275-1288.

Stevens, J. L. and S. M. Day (1985). The physical basis of mb:Ms and variable frequency magnitude methods for earthquakes and explosion discrimination, *J. Geophys. Res., 90*, 3009-3020.

Taylor, S., (1996). Analysis of high-frequency Pg/Lg ratios from NTS explosions and Western U.S. earthquakes, *Bull. Seism. Soc. Am., 86*, 1042-1053.

Taylor, S., A. Velasco, H. Hartse, W. S. Philips, W. R. Walter, and A. Rodgers, (2002). Amplitude corrections for regional discrimination, *Pure. App. Geophys.* (in press).

Walter, W. R., K. Mayeda, and H. J. Patton, (1995). Phase and spectral ratio discrimination between NTS earthquakes and explosions Part 1: Empirical observations, *Bull. Seism. Soc. Am., 85.*, 1050-1067.

Walter, W. R. and M. Ritzwoller, (1998). Summary report of the workshop on the U.S. use of surface waves for monitoring the CTBT, Lawrence Livermore National Laboratory *UCRL-ID-131835*, 16 pp.

Walter, W. R., A. Rodgers, K. Mayeda and S. Taylor (2000). Regional body-wave discrimination research, in the "Proceedings of the 22nd Annual DoD/DOE Seismic Research Symposium, *Dept. of Defense and Dept. of Energy Report, (three volumes),* Volume II, pages 443-452.

Walter, W. R. and S. R. Taylor (2001), A revised Magnitude and Distance Amplitude Correction (MDAC2) procedure for regional seismic discriminants, Lawrence Livermore National Laboratory internal report.

University of California
Lawrence Livermore National Laboratory
Technical Information Department
Livermore, CA 94551